Nondestructive Evaluation of Plasma-Sprayed Thermal Barrier Coatings

D.J. Andrews and J.A.T. Taylor

Acoustic emission has been used as a nondestructive evaluation technique to examine the thermal shock response of thermal barrier coatings. In this study, samples of partially stabilized zirconia powder were sprayed and acoustic emission (AE) data were taken in a series of thermal shock tests in an effort to correlate AE with a given failure mechanism. Microstructural evidence was examined using parallel beam x-ray diffraction and optical microscopy. The AE data are discussed in terms of cumulative amplitude distributions and the use of this technique to characterize fracture events.

Keywords ceramics, nondestructive evaluation, plasma spray, yttria, zirconia

1. Introduction

Nondestructive evaluation (NDE) has become a popular choice in the evaluation of materials and finished products in both the laboratory and the workplace. Time, money, and resources are saved through the use of NDE techniques in combination with destructive characterization tests. Methods such as ultrasonics, thermal wave imaging, and x-ray computed tomography provide information on existing microstructural defects (Ref 1). Acoustic emission (AE) is a nondestructive test that provides information on a structure while it is under stress. It helps describe the dynamic aspects of hidden defects that are contributing to microstructural deformation. The defects that produce AE may or may not be detectable by the other methods listed above. These features of AE make it attractive as a monitoring tool for quality control.

In this study, AE was monitored during thermal shock tests of plasma-sprayed yttria-stabilized zirconia. Thick films of this material are commonly used as thermal barrier coatings (TBCs) in engine applications. They have a lamellar microstructure composed of splats that are mechanically bonded. An intermediate layer, or bond coat, is used to reduce the thermal expansion mismatch between coating and substrate. After thermal cycling, TBCs develop vertical microcracks, which have been shown to improve the thermal shock fatigue of the material (Ref 2). Microcracking is a common AE source due to thermal stress gradients in plasma-sprayed zirconia (Ref 3). Additionally, horizontal crack propagation in the coating and delamination at the bond coat substrate interface can produce spalling, or coating failure. The focus of this study was to use AE to develop a preliminary database of the acoustic response of a TBC. Supported by microstructural evidence, AE could be used as a quality control technique in TBC applications.

2. Experimental Setup

The samples that were used in this experiment were plasma sprayed at Alfred University using a Metco MCN/4MP system. Nickel-chromium alloy straps that measured 300 by 25 by 2 mm were used as substrates. A NiCoCrAlY bond coat was used in conjunction with a yttria (8 wt%) partially stabilized zirconia top coat. The coating covered an approximate area of 100 m by 25 mm on one end of the strap. All the spraying was done in an air atmosphere using argon and hydrogen as the plasma constituents and argon as the powder carrier gas.

Thermal shock tests were performed on three sets of samples. AE was measured by clamping a high-temperature piezoelectric transducer on the unsprayed end of the strap. The strap and transducer arrangement was held in place with a ring stand and clamp while a tube furnace at 1000 °C was rolled onto the strap to provide the thermal shock effect. A schematic of the experimental setup is shown in Fig. 1. A 10 min heat-up stage from room temperature ensued, followed by an air quench back to room temperature (also approximately 10 min).

AE data were read during both the heat-up and quenching stages. A Physical Acoustics Corporation (PAC) LOCAN-AT system was used to collect and process the data. The sensor was a PAC D9215 high-temperature transducer that was used in conjunction with a PAC 1220a preamplifier. The operating parameters included a 60 dB pre-amplification, a gain of 37 dB, and threshold setting of 43 dB.

3. Background Information about AE

AE is a transient elastic wave that is created by energy released from the microstructure of a material that is under stress.

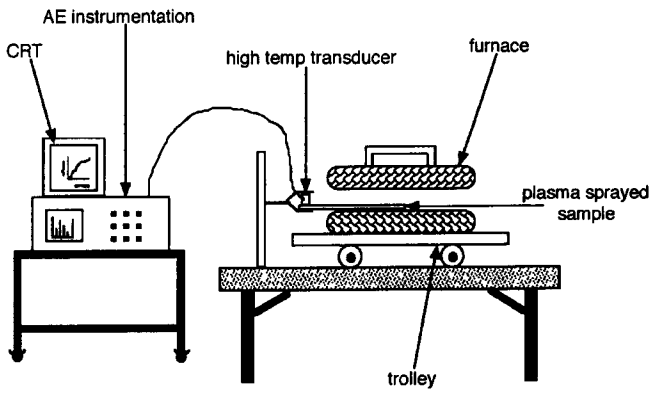

Fig. 1 Experimental setup for measuring AE data from thermal shock tests

D.J. Andrews and **J.A.T. Taylor,** NYS College of Ceramics at Alfred University, Alfred, NY 14802, USA.

In effect, AE is sound waves generated by deformation processes in a material. Classic examples of AE that are detectable by humans are tin cry and the cracking of a pencil as it bends and breaks. Most elastic waves emitted by materials under stress are inaudible to the human ear. However, signals that are out of our hearing range are easily detected by piezoelectric transducers. Transducers are coupled to the sample either directly or via a waveguide. As the elastic wave propagates through the material it produces slight mechanical deformations, which are the phenomena recognized by the transducer. The mechanical pulses are converted to electrical signals that are processed and stored via a microprocessor.

AE signals can be placed in two broad categories: continuous emission and burst-type emission. Continuous emission is typically generated by plastic deformation mechanisms such as multiple dislocation slip (Ref 4). Burst-type emission can result from microcracking in brittle materials, fracture of hard inclusions in alloys, phase transformations, fibers debonding from a matrix, or any other discrete fracture process (Ref 4, 5). The prevailing characteristics of an AE waveform are hits, amplitude, ringdown counts, energy, and duration. An AE waveform is shown in Fig. 2 as a reference (Ref 6). The entire waveform is considered to be a hit. Amplitude is defined as the strongest peak in the waveform. Ringdown counts are the number of times the signal crosses the pre-set threshold for a given hit. Energy is the total energy from the ringdown counts, and duration is the amount of time between the first threshold crossing and the last threshold crossing for a given hit.

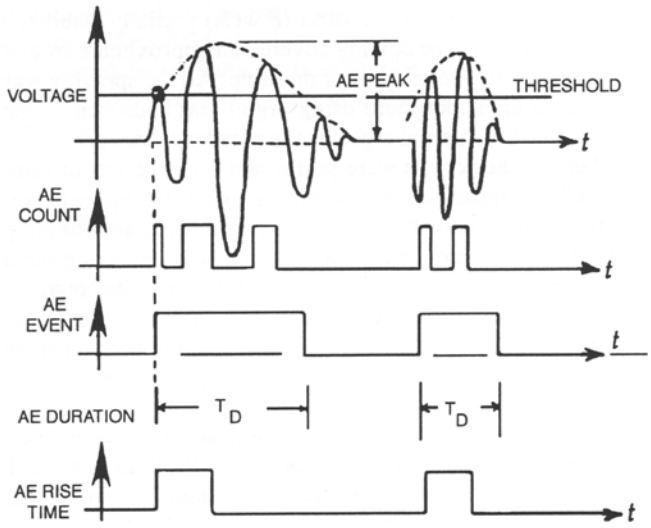

Fig. 2 The characteristics of an AE event. (Source: Ref 6)

Trends in AE data are used to describe the deformation processes for a given material. Amplitude distribution analyses are employed in this study in an attempt to characterize TBCs in terms of AE. Pollock (Ref 7) has summarized four amplitude distribution analyses that may be appropriately applied to AE data. The model that is used here is a cumulative distribution function known as the power law. An implicit assumption in this technique is that the AE response will be burst-type emission (Ref 7). Stated as an equation, the power law is:

$$F(A) = (A/A_t)^{-b}$$

where A is the amplitude for a given hit, A_t is the threshold setting, $F(A)$ is the number of hits with amplitude greater than A, and b is the slope of the curve on log-log axes. After collecting the AE data, the unknown in this equation is b. The magnitude of the b parameter is considered to be a description of the type of fracture mechanism in the material and typically ranges between 0.4 and 4.0 (decades/decade) (Ref 7). A high b value indicates many hits just above the threshold with a lack of high amplitude events. Lower b values indicate a larger proportion of events of higher amplitude.

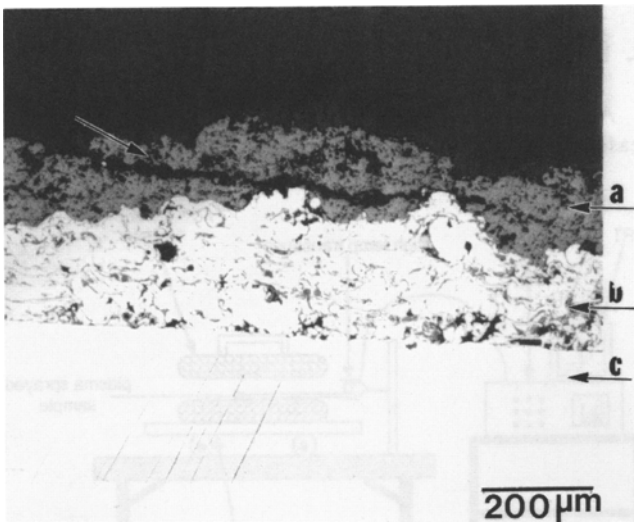

Fig. 3 Cross section of YPSZ coating system. The arrows indicate (a) Y_2O_3 (8 wt%) ZrO_2 TBC, (b) NiCoCrAlY bond coat, (c) nickel-chromium substrate, (d) macrocracking in YPSZ top coat. Differential interference contrast

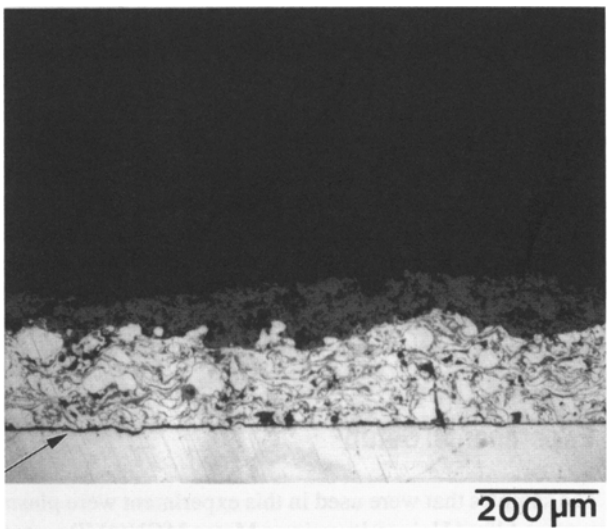

Fig. 4 Delamination of bond coat from substrate as indicated by the arrow in the lower left corner. All other constituents are as labeled in Fig. 3. Differential interference contrast

AE sources that can be expected in plasma-sprayed zirconia are microcracking, phase transformations, and macrocracking. Assuming that a single event corresponds to a single source (neglecting signal interference), then the amplitude of an AE event is related to an isolated source. Microcracking and phase transformations are localized events (within a splat) that are expected to release relatively small bursts of energy. These sources would then produce low-amplitude events. Macrocracking, conversely, is indicative of fracture on a larger scale, such as delamination of the coating from the substrate or crack propagation through the bulk of the coating. Examples of these types of macrocracking are shown in Fig. 3 and 4.

Considering the application of amplitude distributions to the AE data, the magnitude of the *b* parameter should be an indication of the dominant mode of cracking. In TBCs, larger *b* values should indicate a predominance of microcracking and phase transformations. Higher-energy events such as macrocracking and delamination would produce higher-amplitude hits, yielding smaller *b* values (Ref 8).

4. Results

Very few acoustic events occurred during the heat-up stages. The first heat cycle produced the most hits for each sample, but in comparison to the response in the quench stage, the AE in the first part of the cycle was insignificant. During the quench, many hits were registered in the first two minutes, with a smaller number occurring later in the quench stage. Some of the straps had a different response pattern, with nearly half of

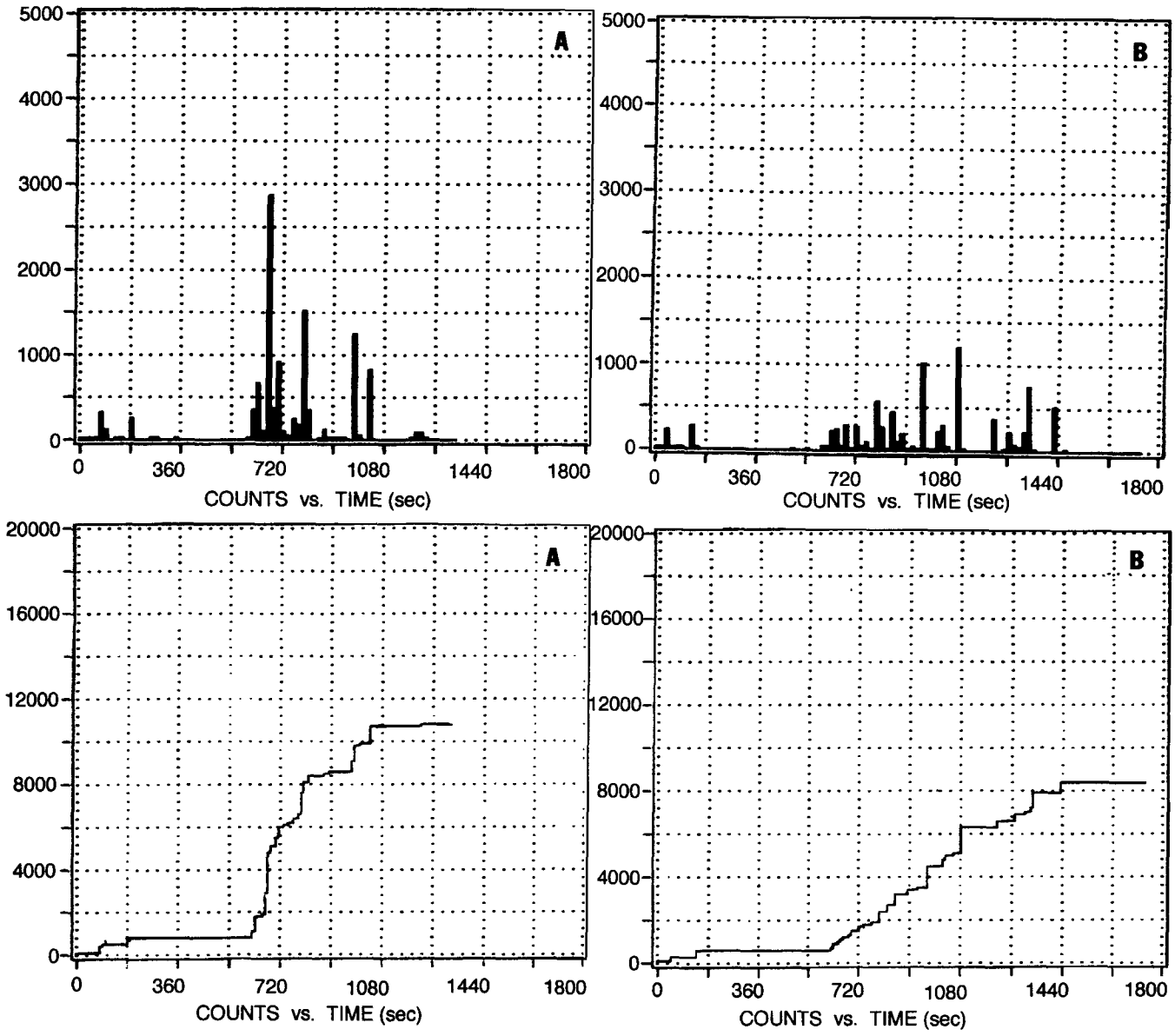

Fig. 5 A comparison of AE response for two different straps showing count rate (top) and cumulative counts versus time (bottom). (a) Strap 1, set 3. (b) Strap 3, set 3

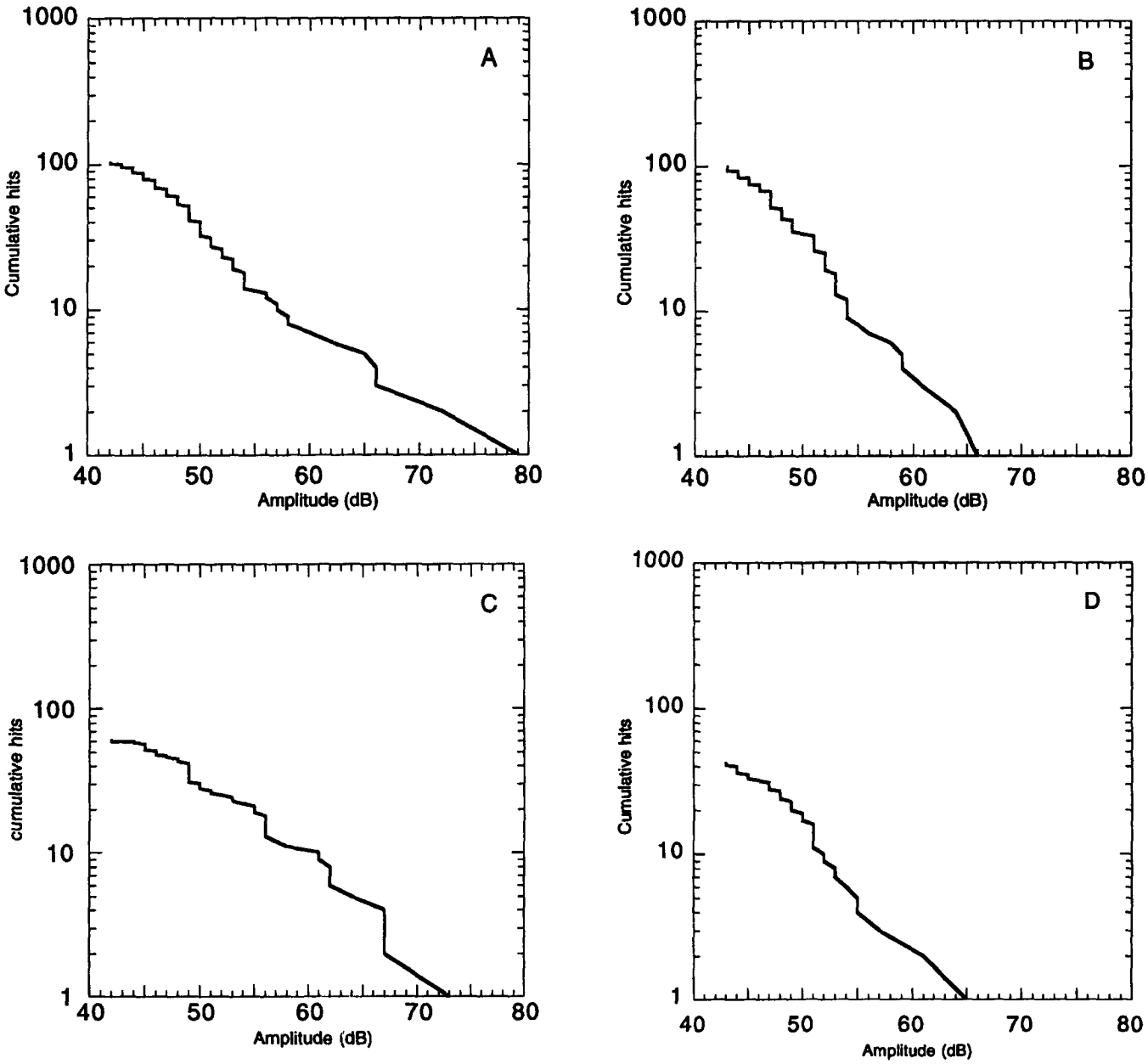

Fig. 6 Cumulative amplitude distributions for the maximum and minimum b values of straps 1 and 3. (a) $b = 1.2$, strap 1 (1st cycle). (b) $b = 1.75$, strap 3 (1st cycle). (c) $b = 0.9$, strap 1 (3rd cycle). (d) $b = 1.2$, strap 3 (2nd cycle).

the hits coming in the very late stages of the cycle. In these cases the sample was near or at room temperature. An example of the difference in behavior is shown in Fig. 5.

The cumulative amplitude distributions of the data produced b values that ranged from 0.9 to 1.75 decades/decade. For a given series of thermal shock cycles, the b parameter generally started at a maximum, dropped to a minimum, and then approached the maximum again. Following the data in Fig. 5, the cumulative distribution functions of straps 1 and 3 are given in Fig. 6. They correspond to the AE from the first two thermal shock cycles for these straps. Apparently, the most severe fracture occurred during the second thermal shock. After that the data indicate a definite trend toward lower amplitude signals in the later thermal shock stages.

It was thought that the late-occurring AE patterns of strap 3 could be the result of a phase change. Straps 1 and 3 were sectioned into three pieces each and parallel beam x-ray diffraction analyses were performed. The x-ray parameters and a typical diffraction pattern is shown in Fig. 7. Small monoclinic peaks were evident for each strap and the overall diffraction patterns were nearly identical. These results were compared to a diffraction pattern from a sample that was sprayed under the same conditions but was not subjected to thermal shock. No significant difference was found between the volume percent of the monoclinic phase of the as-sprayed and post-thermal shock coatings. This eliminated the possibility that a mechanically induced phase change produced significant AE.

Metallographic samples showed differences in the thickness of the coating on each sample and between samples. Some large horizontal macrocracks were found in the coating, with the possibility of spallation shown in Fig. 3. Delamination of the bond coat from the substrate was also seen in some spots (Fig. 4). The large-amplitude hits that occurred in many of the thermal shock cycles could be attributed to failure mechanisms such as these. However, this evidence was found in samples from different straps. Therefore, attributing a difference in *b* values to a specific fracture mode cannot be done at this time with any degree of certainty. It is suspected that the gross crack growth happened in the second and third thermal shock cycles, where the *b* values were the lowest. Subsequent cycles yielded a shift toward lower-amplitude hits, which produced higher *b* values, and would indicate a predominance of microcracking.

5. Summary

AE amplitude distributions were examined in an effort to correlate acoustic response patterns to failure mechanisms in plasma-sprayed yttria-stabilized zirconia TBCs. The acoustic response with respect to time was different in some cases, but the cumulative amplitude distributions followed a similar trend for each sample. Evidence of macrocrack propagation in the top coat and delamination of the bond coat from the matrix was found and is thought to have influenced the lower *b* values (0.9 to 1.2) calculated in the second and third thermal shock cycles. A predominance of microcracking seems to be indicated by the higher *b* values (1.6 to 1.75). This set of *b* values should be taken as the preliminary step in characterizing plasma-sprayed zirconia in terms of AE. Further work is necessary to define the characteristics of TBC in terms of amplitude distributions.

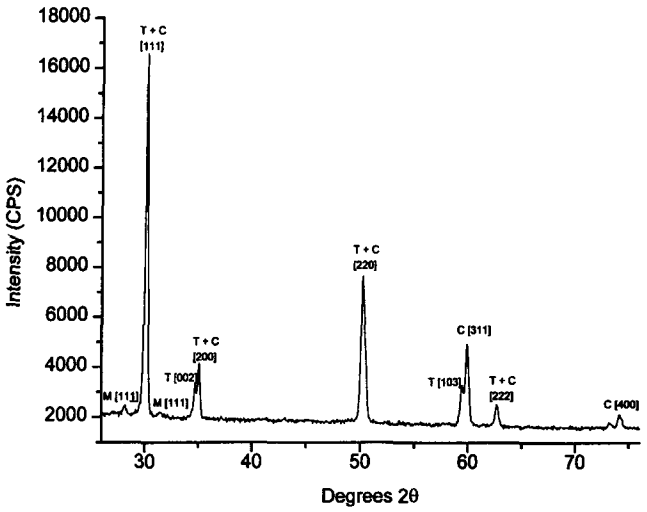

Fig. 7 X-ray diffraction pattern typical of the samples in this experiment. A 2-theta step scan was performed from 10-80° with a step size of 0.05° and a hold time of 5 s.

References

1. L.M. Sheppard, Evolution of NDE Continues for Ceramics, *Am. Ceram. Soc. Bull.*, Vol 70, 1991, p 1265-1279
2. H. Nakahira, Y. Harada, N. Mifune, T. Yogoro, and H. Yamane, Advanced Thermal Barrier Coatings Involving Efficient Vertical Microcracks, *Proc. International Thermal Spray Conf.*, ASM International, 1992, p 519-523
3. N.R. Shankar, C.C. Berndt, H. Herman, and S. Rangaswamy, Acoustic Emission from Thermally Cycled Plasma Sprayed Oxides, *Am. Ceram. Soc. Bull.*, Vol 62, 1983, p 614-619
4. J.R. Matthews, Ed., *Nondestructive Testing Monographs and Tracts*, Vol 2, *Acoustic Emission*, Gordon and Breach Science Publishers, 1983
5. A.A. Pollock, Acoustic Emission Inspection, *Metals Handbook*, 9th ed., Vol 17, ASM International, 1989, p 278-294
6. Y. Hinton, Acoustic Emission, *ASTM Standardization News*, Jan 1995, p 36-39
7. A.A. Pollock, Acoustic Emission Amplitude Distributions, *International Advances in Nondestructive Testing*, Vol 7, 1981, p 215-239
8. D. Almond, M. Moghisi, and H. Reiter, The Acoustic Emission Testing of Plasma-Sprayed Coatings, *Thin Solid Films*, Vol 108, 1983, p 439-447